Radiation Measurements 46 (2011) 1154–1159

Contents lists available at ScienceDirect

Radiation Measurements

journal homepage: www.elsevier.com/locate/radmeas

Measurement of ^{10}B concentration through autoradiography images in polycarbonate nuclear track detectors

A. Portu [a,b], O.A. Bernaola [a], S. Nievas [a], S. Liberman [a], G. Saint Martin [a,*]

[a] Comisión Nacional de Energía Atómica (CNEA), Av. Gral. Paz 1499, AC: B1650KNA, San Martín, Buenos Aires, Argentina
[b] Consejo Nacional de Investigaciones Científicas y Técnicas (CONICET), Rivadavia 1917, AC: C1033AAJ, Ciudad Autónoma de Buenos Aires, Argentina

ARTICLE INFO

Article history:
Received 2 November 2010
Received in revised form
22 July 2011
Accepted 24 July 2011

Keywords:
Boron imaging
BNCT
Autoradiography
Nuclear tracks

ABSTRACT

The determination of the local concentration of boron in the different regions of tissue samples treated by Boron Neutron Capture Therapy (BNCT) could be made through the evaluation of the number of tracks forming autoradiography images. It is necessary to get a "standard" material containing a known amount of ^{10}B, to correlate the number of tracks and boron concentration, i.e. to be used as a reference.

Different systems were tested in order to find a suitable standard. Films made of 2% agarose in boron solutions showed a homogeneous distribution of the ^{10}B atoms in the material structure. This system is easy handled and its physical properties are satisfactory.

On the other hand, a small volume polycarbonate box was designed to contain ^{10}B solutions of known concentration. This system showed a reduced number of background tracks and a promising behavior in many aspects. There is proportionality between track numbers per surface unit and ^{10}B concentration, and between track numbers per surface unit and neutron fluence. Experimental results were compared to calculated values through formulas developed for thick samples autoradiography.

1. Introduction

The capability of Solid State Nuclear Track Detectors (SSNTD) to register damage produced by heavy ions in a permanent way, has converted these materials into a powerful alternative for particle dosimetry. In the years after the first observations by Young (1958), nuclear tracks became the object of many and diverse research works and were also widely applied to a variety of fields.

When an ionizing heavy particle penetrates into a polymeric SSNTD, the ionization and excitation of the material atoms and the subsequent chemical reactions between the produced species may create a damaged zone of the material with broken polymeric chains. Narrow paths are thus formed along the ion's trajectory. These paths can be amplified by etching in an appropriate chemical attack solution, in order to visualize them with an optical microscope (Fleischer et al., 1975). Track pit shape is mainly determined by the ratio (V) between the preferential attack rate V_T along the particle damaged trail and the bulk rate of attack (V_B, etching velocity in the non irradiated material).

If the ionizing particles are generated in "objects" containing heavy ions emitters and put in contact with the detector, an autoradiographic image of the object can be formed there by the produced tracks. This autoradiography image provides relevant information about the spatial distribution of heavy particle emitters in the specimen (Abe et al., 1986).

In particular, it can be used to determine the local distribution of ^{10}B atoms in tissue samples coming from experimental animal models, or even from human patients, to be potentially treated by BNCT. In this case, the samples containing ^{10}B in contact with the detectors must be irradiated with thermal neutrons to yield the capture reaction: $^{10}B(n,\alpha)^{7}Li$. So, the potential track generating particles are: α particle with 1.47 MeV or 1.77 MeV energy (depending on the excitation level), and ^{7}Li ion with 0.84 MeV and 1.02 MeV energy (Table 1). Protons produced in potential capture reactions with ^{14}N atoms in tissue were also included in the table.

The comparison between histological and autoradiography images leads to a qualitative location of the boron atoms in the tissue sample (Altieri et al., 2008; Saint Martin et al., 2007). Moreover, the concentration of ^{10}B in tissue samples may be inferred by measuring the track density in the detector.

Many techniques are applied at present to evaluate the amount of boron in tissue samples from BNCT investigations. Prompt gamma-ray spectroscopy, alpha spectrometry, inductively coupled

* Corresponding author. Tel.: +54 11 6772 7150; fax: +54 11 6772 7188.
E-mail addresses: portu@cnea.gov.ar (A. Portu), bernaola@cnea.gov.ar (O.A. Bernaola), liberman@cnea.gov.ar (S. Liberman), gisaint@cnea.gov.ar (G. Saint Martin).

1350-4487/$ – see front matter © 2011 Elsevier Ltd. All rights reserved.
doi:10.1016/j.radmeas.2011.07.034

Table 1
LET and Range values in polycarbonate were obtained with SRIM-8 (Ziegler et al., 1984)code for particles at initial conditions. V values in polycarbonate were calculated using expressions by Somogyi et al. (1976).

Particle	Energy (keV)	LET (MeVcm^2/mg)	Range (μm)	V
$Alpha_0$	1770	1.6588	8.24	1.400
$Alpha_1$	1470	1.8069	6.769	1.509
Li_0	1016	3.7424	3.815	4.968
Li_1	840	3.5566	3.396	4.437
H+	580	0.3438	9.43	1.005

plasma mass/optical emission/atomic emission spectroscopy (ICP MS/OES/AES) are some examples (Wittig et al., 2008). These methods give the integral value of ^{10}B concentration in the sample. On the other hand, boron concentration can be locally evaluated when autoradiography techniques are applied, which is particularly convenient when the particle emitter is not uniformly distributed in the tissue section.

The following analytical expression, proposed in the literature, relates track density and boron concentration in the sample (Fleischer et al., 1975):

$$\rho = C(B)\frac{N_v \sigma_B \phi}{4}\left(R_\alpha \cos^2\theta_\alpha + R_{\mathrm{Li}}\cos^2\theta_{\mathrm{Li}}\right) \quad (1)$$

where $C(B)$ is the concentration of boron atoms, N_v is the number of atoms per unit volume, σ_B is the neutron capture cross section, and φ is the thermal neutron fluence. R_α, R_{Li} and θ_α, θ_{Li} are ranges and critical angles of the alpha particles and Li fragments respectively. Critical angles refer to the actual possibility of particles to be recorded in the detector and can be calculated in terms of V. Ions entering the detector with angles (measured between the ion's trajectory and the axis normal to the detector surface) larger than the critical angle, are not expected to be preferentially etched. Similar relationships are cited in Armijo and Rosenbaum (1967) and Durrani and Bull (1987).

An alternative approach to assess ^{10}B concentration in a given sample is to use some standard material with a known quantity of ^{10}B as a reference. The standard material (concentration C_s) will produce a track density ρ_s in the area of the detector in contact with it, while a ρ_u track density will be measured in the area of the detector adjacent to the sample under investigation. Taking ratios of these quantities, the unknown concentration can be calculated as shown in Eq. (2).

$$\frac{\rho_u}{\rho_s} = \frac{C_u}{C_s} \quad (2)$$

As the reference system may be used to evaluate samples of materials with composition other than the standard one, it must be assumed that the range (in g cm^{-2}) of the track producing particle in the standard and in the sample is virtually the same (Durrani and Bull, 1987). In fact the medium where the reaction occurs determines the energy loss of the produced particles in their trajectory to the detector surface and consequently the energy they arrive there with. This energy value, together with the incidence angle mentioned before, determine the possibility of observing a track in a certain detector with a given etching process.

Some desirable conditions for a standard in order to be used as a reference for neutron autoradiography are: homogeneous distribution of boron atoms in the material, minimal number of background tracks produced by the material, easy handling, and proportionality of track numbers with ^{10}B concentration and with thermal neutron fluence. Some authors have studied absorbing filter paper (Yanagie et al., 1999), liver homogenate (Fairchild et al., 1986), boron doped Si (Bortolussi, 2007), etc. as standards, and used mainly cellulose nitrate and poly allyl diglycol carbonate (PADC) as track detectors, but not often employed polycarbonate as SSNTD. In this work, different systems were evaluated for their use as standards and calibration curves were obtained for polycarbonate detectors. Experimental results were also studied in relation with analytical expressions proposed in the literature.

2. Materials and methods

Lexan™ polycarbonate films of 250 μm thick were used as SSNTD. Different systems were evaluated for their use as standards:

- Preliminary experiments were performed using absorbing filter paper sheets (AFPS) soaked in borax solutions, as suggested in the previously mentioned literature. Filters of different shapes were used for this purpose: circles ($\varphi = 5$ mm) and rectangles (8 mm × 40 mm). They were stored at −20 °C for 24 h and then adhered on Lexan foils.
- Small boxes (Small Lexan Cases, SLCs) were assembled with Lexan foils. A simple scheme of the construction process is shown in Fig. 1. The two faces were obtained by cutting rectangular shapes of about 25 mm × 15 mm. Two L-shaped pieces were fixed to one face in order to give a thickness of 0.25 mm. The assembly was covered with the other face and all the elements were adhered with polycarbonate–chloroform solution. These boxes are able to contain a volume of about 100 μl. They were filled with ^{10}B solutions (99.99%) of concentrations ranging from 0 to 100 ppm.
- Homogeneous films were fabricated with LMP agarose (Low Melting Point: 65.5 °C, Promega™), in enriched boric acid solutions. Different 2% gels were prepared with ^{10}B concentrations from 0 ppm to 100 ppm. The agarose solutions in their liquid state were poured onto flat plastic molds and then covered with polycarbonate foils. After 24 h, the films were almost solid, so they were separated from the plastic mold. Weight corrections were applied in order to take into account changes in concentration due to evaporation.

Irradiations with thermal neutrons were carried out at the biomedical facility of the RA-3 reactor of the Ezeiza Atomic Center (CAE, Buenos Aires) with fluences of 10^{11} n cm^{-2}, 10^{12} n cm^{-2} and 10^{13} n cm^{-2}. As a matter of routine a calibration with a Self Powered Neutron Detector (SPND) is performed before each irradiation, to ensure that the samples are exposed to the same neutron fluence every time. During the irradiation, the flux is monitored in order to detect any variation that could occur. The fluence is measured with an uncertainty of 8%. More details about thermal neutron field characterization and dosimetry procedures are specified in Miller et al. (2009) and Pozzi et al. (2009).

After the irradiation process, the filters and agarose samples were removed from the polycarbonate detectors, which were etched in PEW alkaline solution (30 g KOH + 80 g ethyl alcohol + 90 g distilled water) at 70 °C for 2 min and then rinsed thoroughly with water. The SLCs were disassembled and the polycarbonate faces were then subjected to the same etching process.

The etching bulk velocity was previously determined by measuring the diameter of fission fragment tracks from a ^{252}Cf source. The obtained value was $V_B = (19.2 \pm 0.6)$ μm h^{-1}. The etching time was chosen in order to obtain an appropriate average track diameter (easily observable), avoiding track overlapping and track density decrease due to layer removal. For that purpose both the track density and track diameter were measured for varying etching time in SLCs samples, corresponding to the 50 ppm and 10^{12} n cm^{-2} condition.

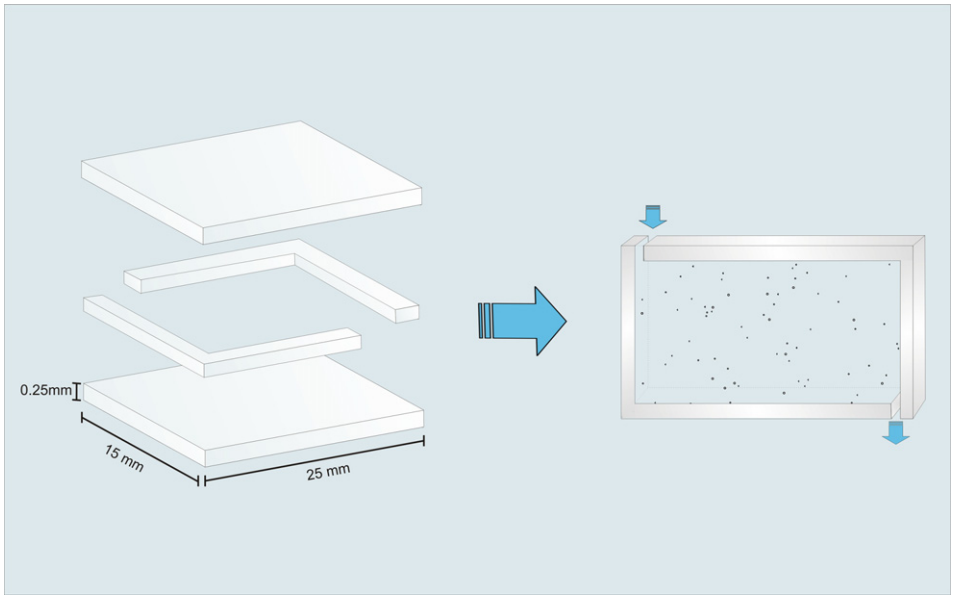

Fig. 1. Small Lexan Cases system (SLCs): scheme of the construction process.

The resulting tracks were observed in a Carl Zeiss MPM 800 digital imaging system (at the Lanais MEF, CNEA-CONICET laboratory). The average number of tracks per surface unit was evaluated by counting over 50 pictures per sample, using image analysis software. Average values of track density were obtained for each concentration and the standard deviation was represented in the figures by the error bars.

The boric acid solutions used for this work were analytically prepared and the concentration values were checked by ICP–OES measurements, performed with a Perkin Elmer Instrument. The digestion and measuring processes were described previously (Liberman et al., 2004).

3. Results and discussion

It has been stated that protons from the reaction $^{14}N(n, p)^{14}C$ are not observed in Lexan at optical microscope level (Apel and Fink, 2004). The *V* value for these protons, whose energy is around 580 keV, is almost equal to 1 under the used etching conditions (Table 1). For this reason, the preferential attack velocity is comparable to the bulk velocity, which prevents proton tracks in this detector from being seen at the light microscope. This characteristic makes this material a suitable SSNTD for its use in tissue neutron autoradiography, since biological samples contain large amounts of N.

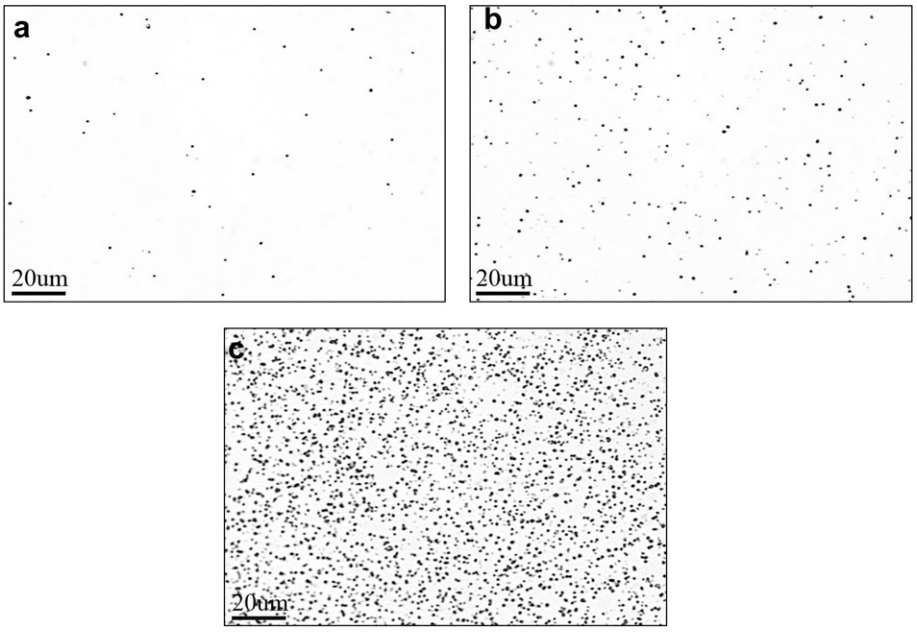

Fig. 2. Light microscope track images obtained with a Carl Zeiss MPM 800 digital imaging system (40X) for the following neutron fluences: a) 10^{11} n cm^{-2}, b) 10^{12} n cm^{-2} and c) 10^{13} n cm^{-2}.

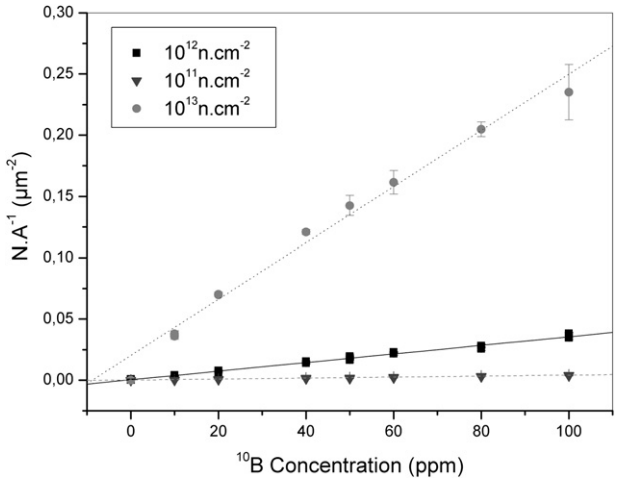

Fig. 3. Track density versus ^{10}B concentration in aqueous solution for 10^{11} n cm^{-2}, 10^{12} n cm^{-2} and 10^{13} n cm^{-2} neutron fluences.

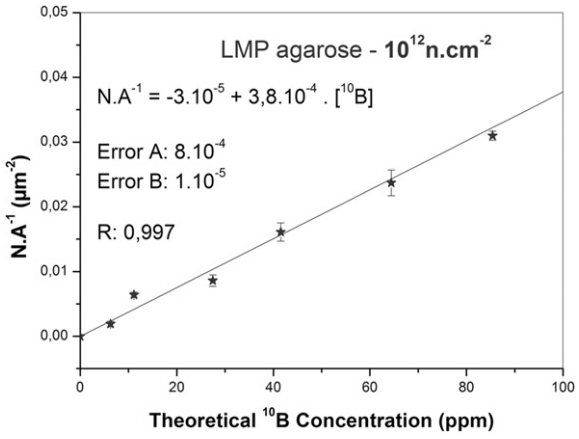

Fig. 4. Calibration curve for LMP agarose films prepared with enriched boron and its corresponding fitting parameters. Fluence 10^{12} n cm^{-2}.

Diameters of tracks produced by both He and Li ions were around 1 µm, after the etching process. These tracks could be clearly observed in the optical microscope, and were counted as a whole to evaluate track density.

Track overlapping was not a major problem in the range of concentrations and fluencies considered. In those cases in which an excessive number of events was observed (concentrations over 50 ppm, irradiated with 10^{13} n cm^{-2}), automatic measurements were checked with manual readings. The amount of boron present in tissue samples (from ^{10}B biodistribution studies) is supposed to be within the analyzed range.

The AFPS autoradiographies showed an increase in track density along the sample's borders. This fact reveals a non uniform distribution of ^{10}B in the filter paper, due to diffusion of the borax solution during the evaporation process. Having observed this behavior in the AFPS, it was decided not to study them any further.

As for the SLCs, reproducible results were obtained with this system. Both faces of the boxes were evaluated for track density and no significant differences were found between them. The tracks were homogeneously distributed on the surface and a reduced number of background tracks was found ($[3.4 \pm 0.5]0.10^{-4}$ µm^{-2}). In Fig. 2a–c), the increase in the number of tracks with neutron fluence can be observed. Proportionality between these two magnitudes was established.

A good linear relationship was also found between the number of tracks per surface unit and the ^{10}B concentration in the solution for a given thermal neutron fluence. Calibration curves displayed in Fig. 3 summarize these facts. Fitting parameters are shown in Table 2.

As it can be inferred from the figures, the results corresponding to 10^{11} n cm^{-2} fluence exhibit the highest deviation, given that the background contribution is more relevant for this condition. A flattening in the 10^{13} n cm^{-2} curve is observed for concentrations over 50 ppm, due to overlapping of tracks. Under these conditions there is a high degree of saturation, which makes individual track counting very difficult. Samples with an excessive quantity of tracks should be measured using other techniques, for example optical densitometry (Portu et al., 2011). Accordingly, the calibration curve for 10^{12} n cm^{-2} was chosen as the most appropriate for quantification purposes, since it combines good statistical results and little track overlapping, which could lead to miscounting.

Table 2
Parameters of the calibration curves obtained for the reference systems. N.A^{-1} = Ord + S.[^{10}B].

System	Fluence (n cm^{-2})	Ord (10^{-5})	S (10^{-5})	R
SLCs	10^{11}	4.59	3.77	0.987
	10^{12}	−4.22	35.6	0.998
	10^{13}	19.7	239	0.990

The autoradiography images of agarose foils also showed homogeneous ^{10}B distribution inside the material's structure and minimal background. The calibration curve displayed in Fig. 4 shows a good linear relationship between ^{10}B concentrations and number of tracks per surface unit.

These track density measurements were also interpolated in the SLCs curves and the ^{10}B concentration results were compared to those obtained by ICP–OES method for the agarose samples. Before interpolation, the track density values were divided by the agarose density (1.03 g cm^{-3}), in order to take into account differences in the material's composition. The evaporation of the agarose films was also considered. The error corresponding to the boron concentration was obtained from the least square approximation equation for the analytical results (Skoog and Leary, 1996).

In Fig. 5, a good accordance is observed between both techniques. Except for the point corresponding to 25 ppm, the differences in the results are not statistically significant in the range

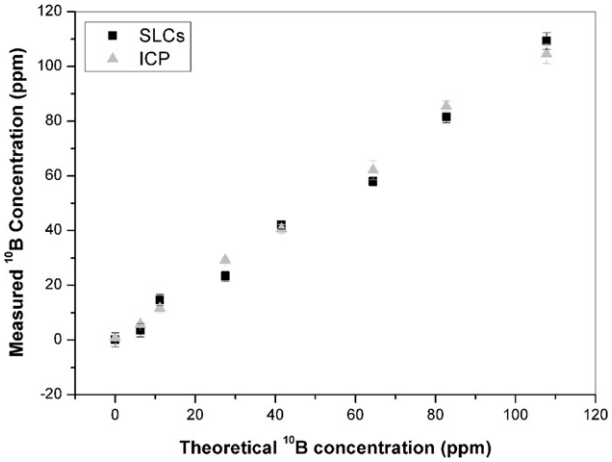

Fig. 5. ^{10}B concentration values obtained for the agarose samples, both with the autoradiography technique and the ICP–OES method.

Table 3
Comparison between experimental (ρ_{exp}) and calculated track density values ($\rho_{eq.1}$ and $\rho_{eq.1,\cos\theta cr\,=\,1}$) for a 50 ppm boron aqueous solution and 10^{12} n cm^{-2} thermal neutron fluence.

	ρ_{exp} ($1/\mu m^2$)	$\rho_{eq.1}$ ($1/\mu m^2$)	$\rho_{eq.1,\cos\theta cr\,=\,1}$ ($1/\mu m^2$)
50 ppm ^{10}B fluence:10^{12}cm^{-2}	0.019 ± 0.002	0.027	0.038

0–40 ppm. This range of concentrations is particularly important, as most of the measured values in clinic and preclinic studies lay in it. This fact validates the autoradiography technique for quantitative determination of ^{10}B.

As mentioned previously, the average values are displayed together with their corresponding standard deviation. However, it has to be noticed that the processes of detection and measurement of tracks involve several parameters whose uncertainties should be propagated. The uncertainty in the fluence is around 8%, but even taking into account other factors as range straggling or counting deviations, the uncertainty for track density is still smaller than 10%.

In Table 3 there is an example of the comparison between experimental and calculated track density values. The measured result was obtained for SLCs filled with a 50 ppm boron aqueous solution and irradiated with 10^{12} n cm^{-2} thermal neutron fluence. In the other columns values calculated with Eq. (1) for these conditions are displayed. The last column shows the result obtained considering cos $\theta_{cr} = 1$ for both particles, which implies no restrictions in the detection of the arriving particles to the detector. Even though in the second column critical angles are considered in the calculation, the experimental value is significantly smaller. This difference could be ascribed to "observation-counting system" sub evaluation, but also to the fact that global critical angles and other approximations are considered in the calculation.

Eq. (1) synthesizes a model that describes the process of particle production and track formation in a simplified way and a perfect match with experimental results should not be expected. In fact, though cited in the literature, in practice authors finally use calibration systems to quantify boron concentration, instead of this expression (Armijo and Rosenbaum, 1967). Other problems, of experimental nature, can be avoided by the use of standards to measure concentrations: sensibility of the observation system and track counting criteria, variable behavior of different plastics, need of absolute neutron fluence measurements, to cite some of them.

In sight of these results and considering that the use of boron doped standards is easier and more consistent to evaluate unknown concentrations in samples, the appraisal of the studied reference systems becomes relevant for further applications.

4. Conclusions

The development and implementation of a procedure based on a "standard" material containing a known amount of ^{10}B to be used as a reference is essential since it is a simple and reliable way to correlate number of tracks and boron concentration.

AFPS showed a non uniform distribution of tracks, probably due to ^{10}B diffusion toward the sample's borders during the drying process.

Calibration curves were constructed for agarose films and SLCs and a good accordance with ICP–OES results was obtained. They will be appropriate to determine boron concentration in a variety of tissue samples whenever the ranges (in g cm^{-2}) of particles generated by the capture reaction are similar in the standard and in the sample. Also, some corrections must be applied when measuring track density from tissue samples. The tissue density and the evaporation coefficient of the sample should be taken into account as corrective factors, to obtain realistic values of concentration. The precision in the results of this technique are smaller than the one for analytical methods, as ICP-OES. The principal advantage of autoradiography is the possibility of obtaining information about the spatial distribution of the emitter element in the unknown sample. In this way, it can be used as a complementary tool for the study of boron uptake in samples from BNCT protocols.

SLCs would constitute the primary system and agarose films could be placed alongside the tissue samples during irradiation. These systems demonstrated the necessary characteristics for use as standards to evaluate the amount of tracks in unknown samples. In future studies these reference systems will be used to determine the boron concentration of tissue samples from preclinical investigations and clinical studies in BNCT.

Acknowledgments

The authors want to thank specially Lic. Silvia Thorp and Lic. Emiliano Pozzi for irradiation in RA 3 reactor facility. We are grateful to Dr. R. L. Cabrini for his useful advice and to Dr. Paola Babay for helping with statistical analysis.

References

Abe, M., Amano, K., Kitamura, K., Tateishi, J., Hatanaka, H., 1986. Boron distribution analysis by alpha-autoradiography. J. Nucl. Med. 27 (5), 677–684.
Altieri, S., Braghieri, A., Bortolussi, S., Bruschi, P., Fossati, F., Pedroni, P., Pinelli, T., Zonta, A., Ferrari, C., Prati, U., Roveda, L., Barni, S., Chiari, P., Nano, R., 2008. Neutron autoradiography imaging of selective boron uptake in human metastatic tumours. Appl. Radiat. Isot 66, 1850–1855.
Apel, P., Fink, D., 2004. Ion track etching. In: Fink, D. (Ed.), Transport Process in Ion Irradiated Polymers, 1st ed. Springer, Berlin.
Armijo, J.S., Rosenbaum, H.S., 1967. Boron detection in metals by alpha-particle tracking. J. Appl. Phys. 38 (5), 2064–2069.
Bortolussi, S., 2007. Boron neutron capture therapy of disseminated tumours. Ph.D. Thesis, Dipartimento di Fisica Nucleare e Teorica, Università degli Studi di Pavia.
Durrani, S.A., Bull, R.K., 1987. In: ter Haar, D. (Ed.), Solid State Nuclear Track Detection. Principles, Methods and Applications. International Series in Natural Philosophy. Pergamon Press, Oxford.
Fairchild, R.G., Gabel, D., Laster, B.H., Greenberg, D., Kiszenick, W., Micca, P.L., 1986. Microanalytical techniques for boron analysis using the ^{10}B(n, alpha)^{7}Li reaction. Med. Phys. 13 (1), 50–56.
Fleischer, R.L., Price, P., Walker, R.M., 1975. Nuclear Tracks in Solids. University of California Press, Berkeley.
Liberman, S.J., Dagrosa, A., Jimenez Rebagliati, R.A., Bonomi, M.R., Roth, B.M., Turjanski, L., Castiglia, S.I., Gonzalez, S.J., Menendez, P.R., Cabrini, R., Roberti, M.J., Batistoni, D.A., 2004. Biodistribution studies of boronophenylalanine–fructose in melanoma and brain tumor patients in Argentina. Appl. Radiat. Isot 61, 1095–1100.
Miller, M., Quintana, J., Ojeda, J., Langan, S., Thorp, S., Pozzi, E., Sztejnberg, M., Estryk, G., Nosal, R., Saire, E., Agrazar, H., Graiño, F., 2009. New irradiation facility for biomedical applications at the RA-3 reactor thermal column. Appl. Radiat. Isot 67 (7–8 Suppl), S226–S229.
Portu, A., Saint Martin, G., Brandizzi, D., Bernaola, O.A., Cabrini, R.L., 2011. ^{10}B concentration evaluation in autoradiography images by optical density measurements: preliminary results. Appl. Radiat. Isot. Ahead of print, doi:10.1016/j.apradiso.2011.04.029.
Pozzi, E., Nigg, D.W., Miller, M., Thorp, S.I., Heber, E.M., Zarza, L., Estryk, G., Monti Hughes, A., Molinari, A.J., Garabalino, M., Itoiz, M.E., Aromando, R.F., Quintana, J., Trivillin, V.A., Schwint, A.E., 2009. Dosimetry and radiobiology at the new RA-3 reactor boron neutron capture therapy (BNCT) facility: application to the treatment of experimental oral cancer. Appl. Radiat. Isot. 67 (7–8 Suppl), S309–S312.
Saint Martin, G., Bernaola, O.A., Tomasi, V.H., Pozzi, E., Thorp, S., Cabrini, R.L., 2007. Aspectos técnicos para la obtención de autorradiografías de cortes de tejido con detectores sólidos de trazas nucleares, XXXIV. Reunión Anual de la AATN, Buenos Aires.
Skoog, D.A., Leary, J.J., 1996. Principles of Instrumental Analysis, 4th ed. Mc. Graw Hill.
Somogyi, G., Grabisch, K., Scherzer, R., Enge, W., 1976. Revision of the concept of registration threshold in plastic track detectors. Nucl. Instrum. Methods 134, 129–141.
Wittig, A., Michel, J., Moss, R.L., Stecher-Rasmussen, F., Arlinghaus, H.F., Bendel, P., Mauri, P.L., Altieri, S., Hilger, R., Salvadori, P.A., Menichetti, L., Zamenhof, R.,

Sauerwein, W.A., 2008. Boron analysis and boron imaging in biological materials for Boron Neutron Capture Therapy (BNCT). Crit. Rev. Oncol. Hematol. 68 (1), 66–90.
Yanagie, H., Ogura, K., Matsumoto, T., Eriguchi, M., Kobayashi, H., 1999. Neutron capture autoradiographic determination of ^{10}B distributions and concentrations in biological samples for boron neutron capture therapy. Nucl. Instrum. Methods Phys. Res. A 424 (1), 122–128.
Young, D.A., 1958. Etching of radiation damage in lithium fluoride. Nature 182, 357–377.
Ziegler, J.F., Ziegler, M.D., Biersack, J.P., 1984. SRIM-2008.4. The Stopping and Range of Ions in Matter 1989, 1998, 2003, 2008.